Scanning tunnelling microscopy of a foldamer prototype at the liquid/solid interface: water/Au(111) *versus* 1-octanol/graphite

Andrey S. Klymchenko,†[a] Norbert Schuurmans,[b] Mark van der Auweraer,[a] Ben L. Feringa,[b] Jan van Esch*[b] and Steven De Feyter*[a]

Received (in Montpellier, France) 30th May 2006, Accepted 9th August 2006
First published as an Advance Article on the web 4th September 2006
DOI: 10.1039/b607660m

We report the design and synthesis of a catechol based foldamer containing amide functionalized alkyl chains, and its monolayer formation at the liquid/solid interface. By scanning tunnelling microscopy, both at the 1-octanol/graphite interface as well as at the water/Au(111) interface, the self-assembly has been investigated with submolecular resolution, demonstrating clear solvent dependent effects on the conformation of the 'foldamer' and its monolayer formation.

Introduction

Control of the lateral assembly and spatial arrangement of micro- and nano-objects at interfaces is often a prerequisite when it comes to potential applications in the field of nano-science and technology. Molecules are the smallest objects which can be ordered by self-assembly on surfaces. In order to exploit such molecular assemblies for catalysis purposes,[1] as (reactive) templates,[2] or in molecular electronics[3] to name a few possible applications, it is absolutely crucial to understand the factors which lead to the two-dimensional self-assembly (often 2D crystallization) of molecules in order to control the outcome of this spontaneous process and to tune the desired properties.

Particularly interesting is the self-assembly of (organic) molecules at the liquid/solid interface which often leads to the formation of physisorbed monolayers.[4] In this respect, the formation of 2D adlayers on surfaces can be compared not only with 3D crystallization but also with, for instance, the formation of 1D systems based upon supramolecular interactions. A first step in the spatial control of molecules on surfaces is controlling their conformation.[5] In many biological systems for example, the exact positioning of functional groups is of key importance for the correct operation of large molecular ensembles. Currently, a lot of research is dealing with artificial foldamers and their self-assembly.[6] These foldamers are designed to fold into a predefined conformation due to specific intramolecular interactions and conformational restrictions. In many instances folding and unfolding can be controlled by tuning of the solvent, showing that also interactions between the foldamers and the solvent are of crucial importance for the conformational preference. Recently, we reported on the successful design of 2D turn mimics based on a catechol bis-amide moiety, that fold into β-turn mimics at the interface of HOPG and 1-octanol as demonstrated by STM.[7] However, it remains unclear to which extend the preference for the folded conformation is influenced by noncovalent interactions with the substrate and the solvent.

Scanning tunnelling microscopy (STM) proves to be an excellent method to probe such layers because of the high spatial resolution (submolecular), its sensitivity to different chemical functionalities, and the non-invasive nature of the experiment.[8] Typically, the substrates are conductive and atomically flat (*e.g.* highly oriented pyrolytic graphite (HOPG), gold, *etc.*). Evidently, the choice of the substrate affects the molecule–substrate interaction and has an influence on the 2D ordering. In addition to the choice of the substrate, also the solvent plays a key role.[9] The solvent can be tuned in function of the particular solute and/or substrate. In case of organic solvents, the solvent has typically a low vapor pressure, is non-conductive, and shows a lower affinity for the substrate than the solute. Such physisorbed systems show adsorption–desorption dynamics at the liquid/solid interface which promotes the repair of defects in the self-assembled layers.[10] Additional control of the monolayer formation can be achieved under potential control in aqueous solutions. In case of physisorbed apolar molecules hydrophobic interactions play a key role, so that the self-assembly could be significantly different as compared to that in organic solvents. Under electrochemical conditions, adsorbate–substrate interactions can be modulated by the surface charge density. Electrochemical environments offer therefore additional possibilities to control surface dynamics and monolayer structure *via* the surface charge and to image those structures by means of electrochemical scanning tunnelling microscopy (EC-STM).[11]

In this contribution, we discuss the self-assembly of a catechol derivative (Fig. 1), by concept related to a previous study,[7] which has been designed to fold on a surface and compare its self-assembly at two different liquid/solid interfaces. The folding of molecule **1** is based upon a functionalized catechol unit. Alkyl chains guarantee the interaction with the

[a] *Department of Chemistry, Laboratory of Photochemistry and Spectroscopy, Institute of Nanoscale Physics and Chemistry, Katholieke Universiteit Leuven, Celestijnenlaan 200-F, 3001 Leuven, Belgium.*
E-mail: Steven.DeFeyter@chem.kuleuven.be; Fax: +32 16 327990
[b] *Stratingh Institute and Material Science Center, University of Groningen, Nijenborg 4, 9747 AG Groningen, The Netherlands.*
E-mail: j.h.van.esch@rug.nl; Fax: +31 50 363 4296
† Present address: Department of Pharmacology and Physical Chemistry, UMR 7175, Institut Gilbert Laustriat, Université Louis Pasteur (Strasbourg I), BP 60024, 67401 Illkirch, France.

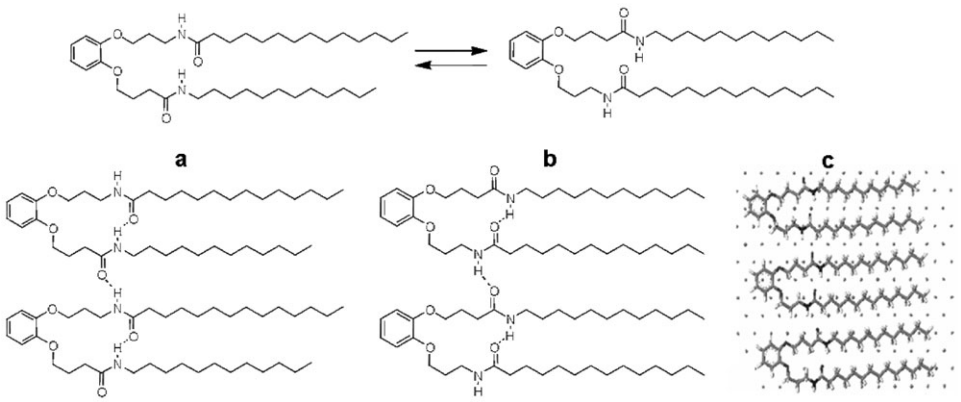

Fig. 1 Chemical structure of **1**, indicating two conformations (A and B) leading to a folded structure. Intra- and intermolecular hydrogen bonding between amide groups is possible in the physisorbed monolayers. (C) Model of a row of **1** on a sheet of graphite based upon molecular mechanics calculations.

substrate and carefully positioned amide groups should both optimize intramolecular hydrogen bonding, leading to an ideal folded structure, and intermolecular hydrogen bonding, leading to 2D crystals. However, in order to realize such assemblies, it is crucial that the molecules indeed adopt the folded conformation they have been designed for and that both alkyl chains of the molecule are adsorbed on the surface.

Results and discussion

Design and synthesis

Despite our previous success in designing a turn element involving the catechol unit,[7] a new design and simpler synthetic approach was followed which should allow a less cumbersome approach for the synthesis of extended foldamers at a later stage. Therefore, from a synthetic point of view, a coupling scheme involving only one building block, with a (protected) acid and a (protected) amine in the same building block is an attractive alternative for the orthogonal protection–deprotection protocol invoked by the previously reported procedure.[7]

The new procedure bears a resemblance to conventional peptide chemistry. In a way the proposed foldamers can be considered as peptidomimetics. In order to be able to follow the procedures of peptide chemistry, a slight modification of the previously reported turn mimic[7] is required.

In the previous foldamer, both amide groups were equivalent (both amides having the carbonyl group connected to the alkyl linker). As a result, to achieve optimized intramolecular hydrogen bonding and alkyl chain conformation, both alkyl chains linking the catechol unit with the amide group differed in length. However, as a result of the new synthetic approach, both amide groups are non-equivalent (they have a reverse orientation), and dissymmetry with respect to the alkyl linkers is no longer an absolute requirement.[7] Both spacers can be of the same length. The total alkyl chain length is also of importance due to the stabilizing effect at the level of the interaction between the molecule and the substrate. Compound **1** was regarded as a good candidate.

Via molecular modeling, it was established that for this molecule conformations allowing for intramolecular H-bond formation are favored and that also intermolecular stabilization *via* van der Waals interactions and H-bonding can be realized (Fig. 1). Two conformers are possible which interconvert by a conformational equilibrium resulting in an overall difference in the length of the molecules of 1.3 Å (2.53 nm (a) *vs.* 2.4 nm (b) in Fig. 1). This small but nevertheless significant difference is due to the dissymmetry in the length of the two groups attached to the catechol moiety.

Compound **1**, with C_3 spacers and C_{12} and C_{13} tails has been synthesized according to Scheme 1. The essential intermediate is highlighted in the scheme. Catechol was reacted with bromo chloropropane to give a mixture of mono- and difunctional chlorides. Extensive column chromatography was necessary to isolate and purify the mono-chloride **2**. It was eventually obtained in 27% yield. Compound **2** was easily converted to the azide **3**, in a modest yield of 53%. Subsequently this compound was converted to the amine (**4**, *via* catalytic hydrogenation, 65% yield). Protection of this amine with benzyl chloroformate was cumbersome and required extensive column chromatography again. The Z-protected amine **5** was eventually obtained in 44% yield. Compound **5** was coupled to methyl bromobutyrate as before, appending the second arm, in 20% yield. The ester **6** was then deprotected by saponification (82%). The Z-protected mono-acid **7** was crystallized. A more advanced protocol for generating the amides was used as described before.[12] The mono-acid was activated with EDC and HOBT, and then reacted with dodecylamine. This reaction generated compound **8** in 35% yield. The Z-protected amine **8** could now be deprotected by catalytic hydrogenation and subsequently reacted with myristic acid, preactivated with EDC/HOBT. This reaction produced compound **1** in 30% yield. All compounds were characterized by ^{1}H-NMR, ^{13}C-NMR and MS.

STM experiments at the liquid/solid interface

The 1-octanol/graphite interface. To reveal the conformation and self-assembly of this molecule, in a first stage, the molecule was dissolved in 1-octanol and a drop of this solution was

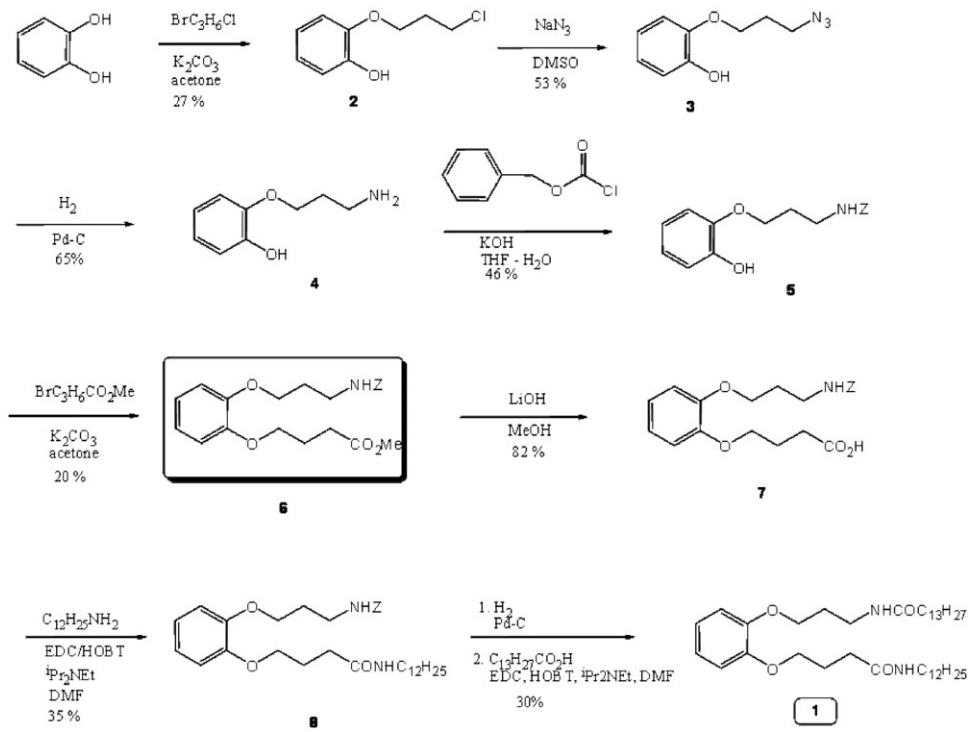

Scheme 1 Synthesis of compound **1**.

applied on a freshly cleaved surface of HOPG. After a while, highly ordered patterns were observed (Fig. 2A). Typically, the 2D patterns showed V shape structures. An accurate analysis of the patterns was possible by calibrating the image based upon the atomic structure of the substrate underneath, which was revealed by lowering the bias voltage, leading to a decreased distance between the tip and the substrate. The distance between the centers of two adjacent rows is 4.5 ± 0.1 nm (double arrow). The distance between equivalent points parallel to the lamella axis is 0.48 nm. The angle between the 'legs' of the V-shaped features and the lamella axis is about 65°. These results are in line with the adsorption of **1** at the liquid/solid interface according to the model indicated in Fig. 2B. The brightest features in the STM image correspond to the location of the aromatic catechol groups (at the position of the arrow heads) while the 'legs' correspond to the alkyl chains containing the amide functions. The amide functions are not well resolved. However, according to the model, intermolecular hydrogen bonding is possible.

For this image type, another possibility was considered where only one alkyl chain for a given molecule was adsorbed while the other one was pointing into the liquid phase. This option, however, was ruled out as far as head-to-head or tail-to-tail arrangements are concerned, based upon the lack of agreement in the dimensions of the molecular model and the STM images.

However, a number of STM images, regularly observed during several measuring sessions at various sites on the substrate, reveal another type of arrangement where a one-chain adsorption is most likely (Fig. 3): the distance between equivalent points in adjacent rows measures ~2.6 nm and the alkyl chains separated by 0.48 nm run perpendicular to the lamella rows. This interpretation is supported by the presence of streaky regions between rows of alkyl chains, suggesting a high degree of mobility which involves the catechol unit and a desorbed alkyl chain. It is very unlikely that solvent molecules (1-octanol) are co-adsorbed, as the length of the 'legs' does not fit with the size of the 1-octanol molecules.[13]

In view of previous results,[7] the lack of folded structures was unexpected. Also modeling (in the absence of solvent) of 5 by 2 clusters on graphite, allowing the alkyl groups to be in epitaxy with the substrate, predicts the foldamer conformation to be thermodynamically more stable than the V-shaped one. As monolayer formation is also affected by kinetic effects, modeling studies have only a limited predictive power. In addition, the solvent, which can not be taken into account in the calculations, can affect the molecular conformation and intermolecular interactions, both in solution and at the liquid/solid interface. Overall, the rate for ordering of these molecules at the 1-octanol/graphite interface was slow (>1 h) and in general, the self-assembled layers could be easily destroyed by the STM tip.

The water/Au(111) interface. Clearly, the 1-octanol/graphite interface is not the appropriate environment to 'stimulate' folding of **1**. Motivated by the solvent dependence of the stability of bisurea-based organogels,[14] revealing an increase in the thermal stability and strength of the gels in going from 1-octanol to 1-propanol due to solvophobic effects, we decided to use ethanol as solvent. Ethanol, however, is not a good solvent for performing STM experiments at the liquid/solid interface due to its high vapor pressure and residual water content.[15] Despite this disadvantage, ethanol can still be used to apply the molecules on a substrate.[16] Thus, the molecules

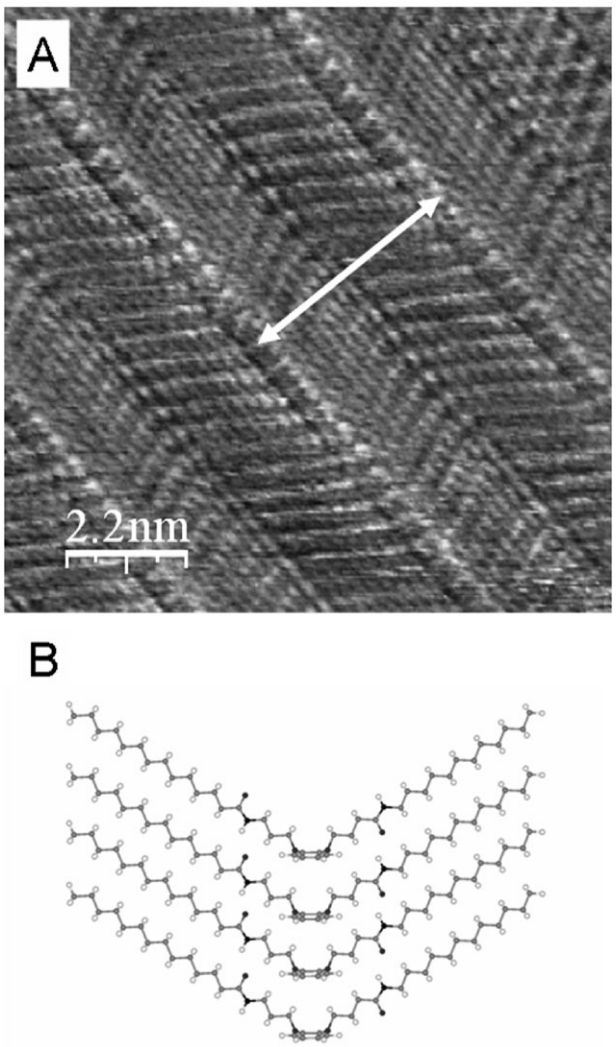

Fig. 2 2D ordering of **1** at the 1-octanol/graphite interface. (A) STM image. I_t = 0.6 nA, V_t = −0.45 V. (B) Tentative molecular model.

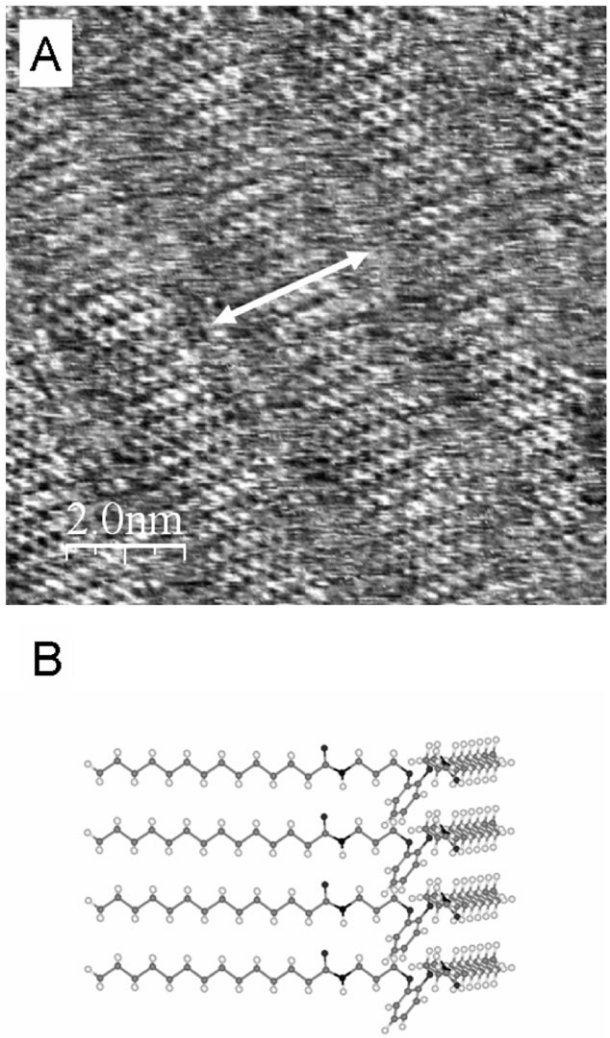

Fig. 3 (A) STM image of a monolayer of **1** at the 1-octanol/graphite interface with only one alkyl chain adsorbed per molecule. I_t = 0.6 nA, V_t = −0.30 V. (B) Tentative molecular model.

were drop-cast from an ethanol solution on Au(111) and the sample was rinsed several times with ethanol to remove the excess of **1** prior to transferring the sample to the electrochemical cell of the EC-STM , which was covered by 0.1 M $HClO_4$ at −100 mV (*vs.* SCE electrode). Au(111) was selected as substrate due to its proven performance in EC-STM experiments.[16] Under these conditions, the molecules are completely insoluble and are fully adsorbed on the gold surface.

Cyclic voltammetry (CV) measurements show an increase of the current at positive voltages as well as shifts of the anion adsorption–desorption peaks (in the region from +100 to +400 mV *vs.* SCE) to higher positive work potentials (Fig. 4), which confirms the presence of the adsorbate on Au(111). We did not perform scans at higher work potentials in order to avoid possible electrochemical oxidation of the catechol residue of molecule **1**.

By EC-STM, ordered structures were observed only at potentials below +100 mV (*vs.* SCE), while at higher potentials disordered aggregates of molecules were detected (not shown). All the EC-STM measurements were performed at a work potential of −100 mV (*vs.* SCE), which was fixed *after* recording the corresponding CV curves. Therefore, we expect that the ordered layers observed in the present study are formed after the potential was fixed at −100 mV.

In comparison to the 1-octanol/graphite interface, monolayers are much more stable and less dynamic (at least at the work potential of −100 mV *vs.* SCE), most likely due to the hydrophobic effect.

STM images reveal several two-dimensional polymorphs. One of them resembles the V-shaped structures observed at the 1-octanol/HOPG interface. Indeed, the lamellae are composed of bright features and each of them has two chains (Fig. 5A and Fig. 6A). However, the angle between the chains is larger, *ca.* 150° and the lamellae are not straight but wavy.[17]

Another monolayer structure (Fig. 5B and 6B), which was also frequently observed on the same sample but at different locations, is characterized by perfectly aligned lamellae formed by perpendicularly oriented alkyl chains. Moreover, we observe single and double rows of bright spots. The distance

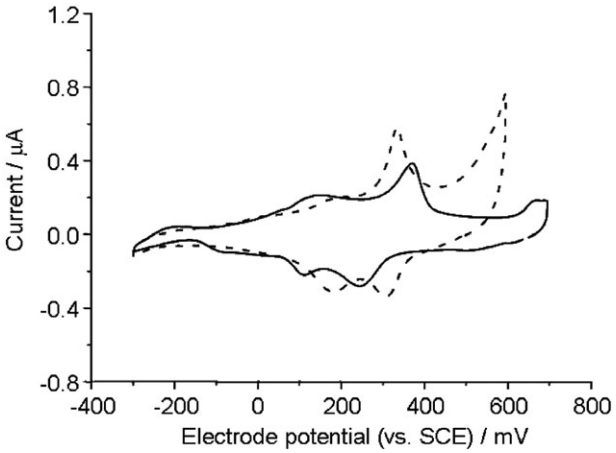

Fig. 4 CV curves of bare Au(111) in 0.1 mM $HClO_4$ (solid line) and in presence of adsorbed molecule **1** (dashed line). Note that both curves were obtained in different experimental sessions.

between the bright spots (catechol groups) is $\sim$1.0 nm, which is two times as large as the distance between the alkyl chains. This kind of packing is clear evidence that the molecules fold and form lamellae *via* a head-to-head arrangement (Fig. 6B). In addition to the head-to-head arrangement, we also observe head-to-tail arrangements of folded molecules (Fig. 5C, D and 6C). The latter indicates the absence of a specific interaction between lamellae. Some alkyl chains appear longer than others and some lamellae differ slightly in width by about 0.15 nm, which corresponds well to the difference expected based upon the two possible folded conformations (Fig. 1). Despite this observation, no firm conclusions can be drawn regarding the specific conformation of the molecules, except for the fact that upon folding, intramolecular hydrogen bonding is optimized.

No indication was found that molecules adsorb with only one alkyl chain on the substrate. The molecules are always adsorbed with both alkyl chains adsorbed on the substrate, often adopting a folded conformation. This folded conformation can intuitively be understood due to the solvophobic effect of the aqueous subphase. By bringing these molecules, which are water-insoluble, at the water/gold interface, we have restricted the number of unfolded conformations. Note that at this stage we have not investigated specifically the influence of the substrate (graphite *versus* Au(111)) which should, in general, not be neglected. For instance, the angle between the alkyl chains of the V-like structures is larger on Au(111) and molecules are less well aligned. A full investigation of different

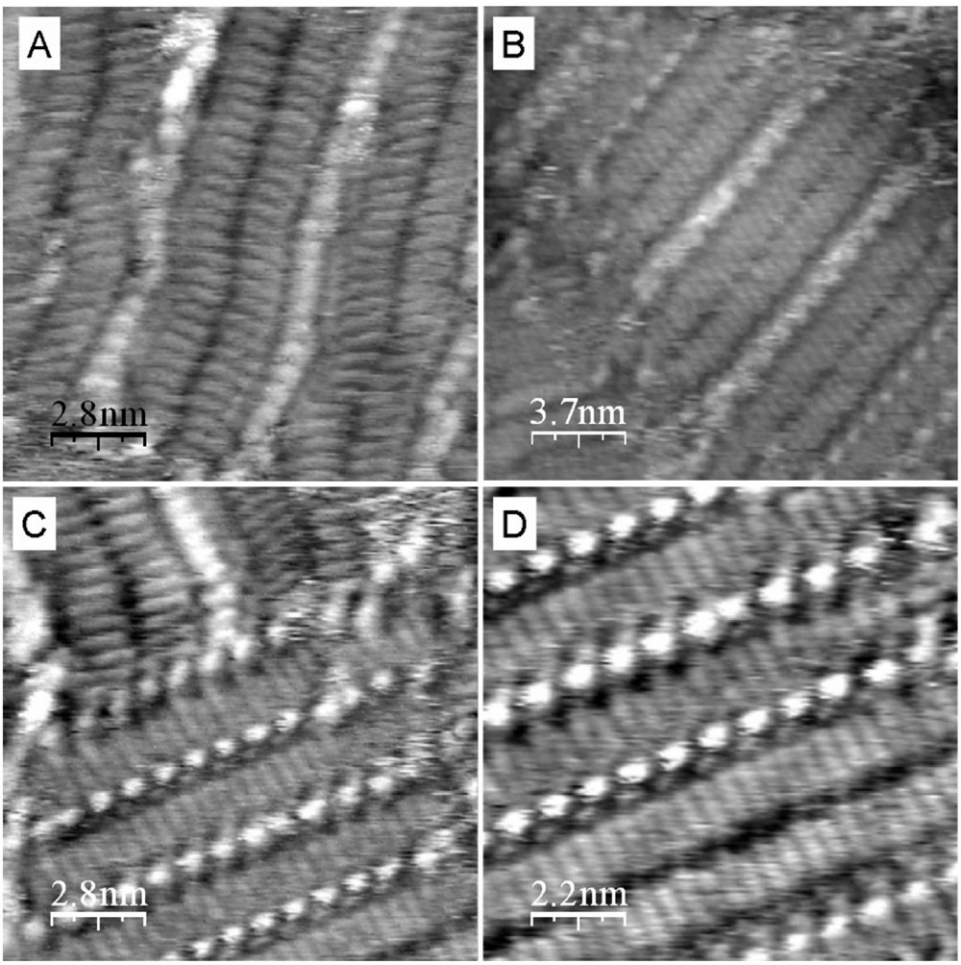

Fig. 5 EC-STM images of molecular ordering of **1** on Au(111) in 0.1 mM $HClO_4$. (A) $V_W = -100$ mV (*vs.* SCE), $V_t = -500$ mV, $I_t = 1$ nA. (B–D) $V_W = -100$ mV (*vs.* SCE), $V_t = -600$ mV, $I_t = 1$ nA.

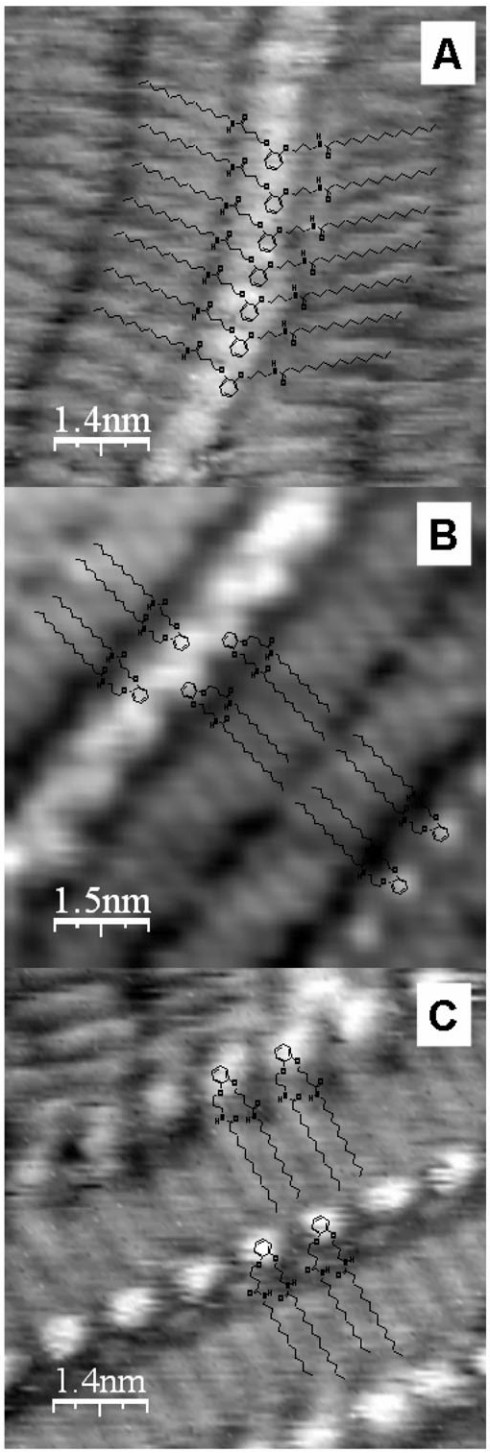

Fig. 6 Zoomed STM images of (A) Fig. 5A, (B) Fig. 5B, and (C) Fig. 5C with tentative molecular models of the molecular packing.

solvent-substrate combinations will be necessary to get a conclusive answer on the relative importance of solvent *versus* substrate. However, we believe that it is mainly the choice of solvent—the solvophobic effect—which for this particular system is the driving force for molecular folding. It is unlikely that a 'conformational memory effect' (solvophobic interaction in ethanol) alone is responsible for the folded conformation observed by EC-STM. Prior to imaging, the formation of an adsorbate layer is checked by taking a CV curve. During the recording of the voltammogram, at high positive potentials, the highly ordered phase is destroyed possibly also affecting the molecular conformation.

Conclusion

In conclusion, the water/Au(111) interface proves to be a good environment to support the folding of water-insoluble catechol type foldamers and their ordering into 2D patterns, which has been revealed by EC-STM under potential control. Folding of the present molecule is driven by a combination of solvophobic and H-bonding interactions, which is analogous to folding of biomolecules in aqueous media, and is as such promoted at the water/substrate interface. In general, electrified surfaces hold great promises to (affect) the conformation/ordering of molecules, not only water-soluble ones, but also water-insoluble ones, which opens many possibilities for applications.

Experimental

Synthesis

All solvents were dried according to standard procedures. Starting materials were purchased from Aldrich or Acros. ^{1}H-NMR spectra were recorded on a Varian VXR-400 spectrometer (at 100.57 MHz) in $CDCl_3$ chemical shifts are given in ppm relative to $CDCl_3$ (7.24). ^{13}C-NMR spectra were recorded on a Varian VXR-400 spectrometer (at 400 MHz) in $CDCl_3$, chemical shifts are given relative to $CDCl_3$ (77). The splitting patterns in the ^{1}H-NMR spectra are designated as follows: s (singlet), d (doublet), t (triplet), m (multiplet), br (broad). Melting points were measured on Stuart scientific SMP1 apparatus. HRMS was performed on a JEOL JMS 600H spectrometer in EI+ ionization mode.

General procedure for the amide couplings. The carboxylic acids were dissolved in DMF. To the solutions was added one equiv. of diisopropylethyl amine. The mixtures were stirred and were cooled to 0 °C. HOBT (hydroxybenzotriazole) and EDC (a water soluble version of DCC) were added in equimolar amounts. The mixtures were stirred for 10 min and the amines were added. The mixtures were stirred for 24 h at room temperature. The mixtures were evaporated *in vacuo* at 40 °C. CH_2Cl_2 and water were added. The organic phase was extracted with water, dilute HCl (aq) and again water. The organic phase was dried on Na_2SO_4 and evaporated *in vacuo*. The crude products were further purified by column chromatography (silica, 2% MeOH in $CHCl_3$). The amides were the first fractions to come off the column.

General procedure for the Z-deprotections. The Z-protected amines were dissolved in MeOH. A balloon filled with H_2 gas was mounted on the flask. A small amount of Pd–C (10%) was added to the solution. The flask was evacuated, filled with hydrogen, again evacuated, and brought under H_2 atmosphere again. The mixtures were stirred for 12 h. Upon removal of the balloon, the catalyst was filtrated over celite, and the filtrate

was evaporated. The amines were used without further purification.

2-(3-Chloro-propoxy)-phenol (2). Catechol (100 g, 0.9 mol) was dissolved in acetone (500 ml) and the solution was stirred at reflux. Pre-dried (120 °C) K_2CO_3 (100 g, 0.72 mol) was slowly added to the stirred solution, which got a dark color. The mixture was stirred for 10 min and bromo chloropropane (120 g, 0.76 mol) was added dropwise. The mixture was stirred at reflux for 48 h. The mixture was filtered hot and the residue was concentrated *in vacuo*. $CHCl_3$ (250 ml) was added, this mixture was stirred and filtrated again. The crude product was purified by trituration with pentane. The product separated as a yellow oil. This was collected and further purified by column chromatography (silica, $CHCl_3$). Yield: 45 g (0.24 mol, 27%). ^{1}H-NMR ($CDCl_3$): δ_H 6.80–6.87 (4H, m, $H_{Aromatic}$)(1H, s, OH), 4.16 (2H, t, ^3J = 5.9 Hz, OCH_2), 3.68 (2H, t, ^3J = 6.2 Hz, CH_2Cl), 2.23 (2H, m, $CH_2CH_2CH_2$). ^{13}C-NMR ($CDCl_3$): δ_C 121.8, 120.2, 114.7, 111.9, 65.5 (OCH_2), 41.3, 32.0. MS (CI^+): *m*/*z* 187 (M^+, 29), 110 (100). HRMS: calcd for $C_9H_{11}ClO_2$: 186.045, found 186.051.

2-(3-Azido-propoxy)-phenol (3). Compound **2** (44 g, 0.24 mol) was dissolved in DMSO (300 ml). The mixture was stirred and NaN_3 (20 g, 0.3 mol) was added in small portions. The mixture was stirred at 60 °C for 12 h. The mixture was then poured into water (500 ml), and extracted with EtOAc (2×). The organic layers were washed with water (2×), dried (Na_2SO_4) and concentrated *in vacuo* to yield the product as a yellow oil. It was purified by trituration with pet. ether. Yield: 25 g (0.13 mol, 53%). ^{1}H-NMR ($CDCl_3$): δ_H 6.84–6.91 (4H, m, $H_{Aromatic}$), 5.69 (1H, s, OH), 4.12 (2H, t, ^3J = 6.0 Hz, OCH_2), 3.50 (t, ^3J = 6.6 Hz, 2H, CH_2N_3), 2.07 (m, 2H, $CH_2CH_2CH_2$). ^{13}C-NMR ($CDCl_3$): δ_C 121.6, 120.3, 117.2, 111.7, 68.2, 44.0, 32.0. HRMS: calcd for $C_9H_{11}N_3O_2$ 193.085, found 193.089.

2-(3-Amino-propoxy)-phenol (4). The azide **3** (24 g, 0.12 mol) was dissolved in MeOH (100 ml) in a two-necked flask equipped with a balloon filled with H_2. A small amount (100 mg) of palladium on carbon (Pd–C, 10%) was added. After evacuating, the mixture was stirred under H_2-atmosphere for 12 h at room temperature. The catalyst was removed by filtration over celite and the filtrate was concentrated *in vacuo*. The amine was obtained as an oil, that waxified on standing. Yield: 13 g (78 mmol, 65%). ^{1}H-NMR ($CDCl_3$): δ_H 6.81–6.92 (4H, m, $H_{Aromatic}$), 5.81(2H, br, OH) 4.01 (2H, t, ^3J = 5.1 Hz, OCH_2), 3.02 (2H, m, CH_2NH_2), 1.96 (2H, m, $CH_2CH_2CH_2$). ^{13}C-NMR ($CDCl_3$): δ_C 125.0, 120.3, 119.7, 117.7, 73.0, 39.8, 31.4.

[3-(2-Hydroxy-phenoxy)-propyl]-carbamic acid benzyl ester (5). The amine **4** (12 g, 72 mmol) was dissolved in THF–H_2O (5 : 1, 200 ml). The mixture was cooled to 0 °C and KOH (30 g, 0.2 mol, excess) was added. The mixture was stirred for 5 min and benzyl chloroformate (12.5 ml, 15 g, 85 mmol, 1.2 eq.) was added drop-wise. The mixture was stirred for 2 h at 0 °C, and allowed to stand overnight at room temperature. Water (100 ml) was added, and the organic layer was separated. The aqueous layer was extracted with CH_2Cl_2 (3×). The combined organic layers were dried and concentrated *in vacuo*. The compound was purified by column chromatography (silica, $CHCl_3$ + 5% MeOH). Yield: 10 g (33 mmol, 46%). ^{1}H-NMR ($CDCl_3$): δ_H 7.32 (5H, m, $H_{Aromatic}$ of the benzyl group), 6.73–6.85 (4H, m, $H_{Aromatic}$ of the catechol moiety), 5.43 (1H, br, OH), 5.02 (2H, s, $NHCO_2CH_2C_6H_5$),3.96 (2H, t, ^3J = 5.8 Hz, OCH_2), 3.31 (2H, t, ^3J = 4.8Hz, CH_2NHCO_2), 1.87 (2H, t, ^3J = 6.2 Hz, $CH_2CH_2CH_2$). ^{13}C-NMR ($CDCl_3$): δ_C156.7, 148.1, 145.7, 128.3, 128.0, 121.7, 119.9, 115.1, 112.7, 67.3, 66.1, 39.1, 29.4. MS (EI^+): *m*/*z* 301 (M^+, 10%), 192 (20). HRMS: calcd for $C_{17}H_{19}NO_4$: 301.131, found 301.139.

4-[2-(3-Benzyloxycarbonylamino-propoxy)-phenoxy]-butyric acid methyl ester (6). The Z-protected amine **5** (9 g, 30 mmol) was dissolved in acetone (250 ml). The mixture was stirred and pre-dried K_2CO_3 (6.2 g, 45 mmol) was added portion-wise. The mixture was stirred for 30 min at reflux temperature and methyl bromobutyrate (6.5 g, 36 mmol, 1.2 eq.) was added slowly. The mixture was stirred at reflux for 72 h. The mixture was filtered hot and the residue was concentrated *in vacuo*. $CHCl_3$ was added, and this mixture was stirred and filtrated again. The filtrate was concentrated *in vacuo* and subjected to extensive column chromatography (3×: silica, $CHCl_3$; EtOAc; $CHCl_3$ + 5% MeOH + 1% NH_3). Yield: 2.4 g (6 mmol, 20%). ^{1}H-NMR ($CDCl_3$): δ_H7.35 (5H, m, $H_{Aromatic}$ of the benzyl group), 6.88–6.92 (4H, m, $H_{Aromatic}$ of the catechol group), 5.02 (2H, s, $NHCO_2CH_2C_6H_5$) 4.08 (2H, t, ^3J = 5.7 Hz, $OCH_2C_2H_4NHCO_2$), 3.97 (2H, t, ^3J = 5.8 Hz, $OCH_2C_2H_4CO_2Me$), 3.65 (3H, s, CO_2CH_3), 3.42 (2H, m, CH_2NHCO_2), 2.26 (2H, t, ^3J = 7.3 Hz, $CH_2CO_2CH_3$), 1.84 (4H, m, 2× $CH_2CH_2CH_2$) ^{13}C-NMR ($CDCl_3$): δ_C156.0, 149.1, 145.8, 128.3, 127.7, 122.2, 117.8, 115.2, 72.6, 67.5, 66.2, 52.2, 39.1, 29.4, 25.8.

4-[2-(3-Benzyloxycarbonylamino-propoxy)-phenoxy]-butyric acid (7). The ester **6** (2.5 g, 6 mmol) was dissolved in MeOH (50 ml) and LiOH (200 mg) was added. The mixture was stirred for 2 h at room temperature. The mixture was concentrated *in vacuo* and CH_2Cl_2 was added. The resulting suspension was acidified with HCl (g), *in situ* generated by carefully adding H_2SO_4 to HCl (aq). The Li salts precipitated and were removed by filtration: the filtrate was concentrated *in vacuo* to give the acid as a white solid. Yield: 1.9 g (4.9 mmol, 82%). Mp 195–196 °C (from $CHCl_3$). ^{1}H-NMR confirmed removal of the methoxy group. MS (EI^+): *m*/*z* 387 (M^+, 5%), 192 (51). HRMS: calcd for $C_{21}H_{25}NO_6$ 387.168, found 387.171.

{3-[2-(3-Dodecylcarbamoyl-propoxy)-phenoxy]-propyl}-carbamic acid benzyl ester (8). Compound **7** (mono-Z protected acid, 200 mg, 0.5 mmol) was dissolved in DMF (20 ml). The solution was stirred and diisopropylethylamine (DIEA, Hunig's base, 100 µl) was added. The solution was stirred for 10 min at room temperature. EDC (1-(3-dimethylamino-propyl)-3-ethylcarbodiimide hydrochloride, 100 mg, 0.55 mmol) and HOBT (hydroxybenzotriazole, 90 mg, 0.6 mmol) were added and the mixture was stirred for 30 min. Dodecylamine (100 mg, 0.55 mmol) was added and the mixture was stirred for 24 h at room temperature. The mixture was concentrated *in vacuo* at 80 °C and $CHCl_3$ (50 ml) was added. This

solution was extracted with water, HCl (aq. 0.6 M) and again water. The aqueous layers were extracted with $CHCl_3$. The combined organic layers were dried (Na_2SO_4) and concentrated *in vacuo*. The crude product was purified by column chromatography (silica, $CHCl_3$ + 5% MeOH). Yield: 90 mg (0.16 mmol, 35%). ^{1}H-NMR: δ_H 7.26–7.24 (5H, m, $H_{Aromatic}$ of the benzyl group), 6.77–6.81 (4H, m, $H_{Aromatic}$ of the catechol group), 5.99 (1H, br, CO*NH*), 5.98 (1H, br, *NH*CO_2CH_2), 5.00 (2H, s, $NHCO_2CH_2C_6H_5$), 3.98 (2H, t, ^3J = 5.6 Hz, $OCH_2C_2H_4NHCO_2$), 3.89 (2H, t, ^3J = 5.7 Hz, $OCH_2C_2H_4CONH$), 3.38 (2H, m, $CONHCH_2$), 3.05 (2H, m, CH_2NHCO_2), 2.19 (2H, t, ^3J = 7.3 Hz, CH_2CONH), 1.94 (4H, m, 2× $CH_2CH_2CH_2$), 1.60 (2H, m, $CONHCH_2CH_2$), 1.16 (18H, m, $(CH_2)_9$), 0.82 (3H, t, ^3J = 6.4 Hz, CH_2CH_3). ^{13}C-NMR: δ_C 172.7, 156.8, 148.9, 148.5, 136.8, 128.8, 128.7, 121.8, 121.2, 113.6, 113.4, 67.8, 66.9, 65.4, 40.2, 39.7, 33.0, 32.2, 30.0, 29.9, 29.8, 29.8, 29.7, 29.3, 28.0, 27.2, 26.8, 25.4, 23.0, 14.4. MS (EI^+): *m*/*z* 554 (M^+, 1%), 254 (100).

Tetradecanoic acid {3-[2-(3-dodecylcarbamoyl-propoxy)-phenoxy]-propyl}-amide (1). Compound **8** (80 mg) was dissolved in MeOH (20 ml). The solution was placed in a 2-necked flask, mounted with a balloon filled with H_2 gas. Pd–C (10%, 50 mg) was added. After evacuation the solution was stirred for 12 h. under H_2 atmosphere. The catalyst was removed by filtration over celite, the filtrate concentrated *in vacuo*. ^{1}H-NMR confirmed removal of the Z-group. Yield: 60 mg. The free amine was coupled to myristic acid (60 mg) as described above, activating the acid with EDC (60 mg), HOBT (50 mg) and DIEA (60 µl). Yield: 25 mg (0.04 mmol, 30% over 2 steps). ^{1}H-NMR: δ_H 6.85–6.95 (4H, m, $H_{Aromatic}$ of the catechol moiety), 4.04 (2H, t, ^3J = 3.4 Hz, OCH_2), 4.02 (2H, t, ^3J = 2.6 Hz, OCH_2), 3.51 (2H, m, $OC_2H_4CH_2NHCO$), 3.19 (2H, m, $CONHCH_2$), 2.45 (2H, t, ^3J = 8.3 Hz, $OC_2H_4CH_2CONH$), 2.16 (2H, m, $NHCOCH_2$), 1.98 (4H, t, ^3J = 5.8 Hz, 2× $CH_2CH_2CH_2$), 1.58 (2H, m, $CONHCH_2CH_2$), 1.43 (2H, m, $NHCOCH_2CH_2$), 1.22 (m, 38H, $(CH_2)_9$ + $(CH_2)_{10}$), 0.86 (6H, t, ^3J = 6.4 Hz, 2× $CH_2CH_2CH_3$). ^{13}C-NMR: δ_C 179.1, 174.7, 149.6, 122.6, 122.5, 115.0, 114.9, 69.2, 68.9, 38.9, 37.8, 35.1, 33.0, 31.5, 30.7, 30.6, 30.6, 30.5, 30.4, 30.4, 30.3, 30.2, 29.9, 26.9, 25.9, 25.6, 23.7, 15.1. MS (Maldi-TOF): calcd. 631, found: 631. HRMS: calcd for $C_{39}H_{70}N_2O_4$ 630.984, found 630.991.

Scanning tunnelling microscopy

STM experiments at the 1-octanol/graphite interface were performed using a Discoverer Scanning Tunnelling Microscope (Topometrix Inc., Santa Barbara, CA) along with an external pulse/function generator (Model HP 8111 A), with negative sample bias. Tips were electrochemically etched from Pt–Ir wire (80% : 20%, diameter 0.2 mm) in 2 M KOH : 6 M NaCN solution in water. Prior to imaging, the compound under investigation was dissolved in 1-octanol at a concentration close to saturation, and a drop of the solution was applied onto a freshly cleaved surface of highly oriented pyrolytic graphite (HOPG, grade ZYB, Advanced Ceramics Inc., Cleveland, OH). Then, the STM tip was immersed in the solution and images were recorded at the liquid/solid interface. The STM images were acquired in the variable-current mode (constant height). The measured tunnelling currents are converted into a gray scale: black (white) refers to a low (high) measured tunnelling current. For analysis purposes, recording of a monolayer image was followed by imaging the graphite substrate underneath under the same experimental conditions, except if stated otherwise.

EC-STM experiments have been performed using a home-built STM setup designed and constructed in the group of Prof. Klaus Wandelt (University of Bonn).[18] The instrumental design allows performing simultaneously cyclic voltametry (CV) and STM measurements. A platinum wire was used as a pseudo-reference electrode, while all potentials were rescaled to the saturated calomel electrode (SCE) reference electrode. Prior to each STM experiment, a Au(111) single crystal (MaTeck company, Julich, Germany) was electrochemically etched and flame annealed. For this purpose, the Au(111) crystal was immersed into 0.1 M sulfuric acid and an anodic potential of 10 V was applied between the crystal and a platinum foil for about 30 s. Then, after rinsing with Milli-Q water (Milli-Q purification system >18 MΩ cm) the sample was immersed into 0.1 M hydrochloric acid in order to reduce the Au(111) surface. Again, the Au substrate was rinsed with Milli-Q water and flame annealed for another 2 min. To deposit **1** on the gold substrate, a drop of an ethanol solution of **1** (1 mg ml^{-1}) was placed on the Au(111) surface. After solvent evaporation the surface was thoroughly rinsed with ethanol and dried. EC-STM imaging was started after completion of the *in situ* CV measurements. The STM tips were electrochemically etched from a 0.25 mm tungsten wire in 2 M KOH solution and subsequently isolated by passing the tip through a drop of hot-glue. The EC-STM measurements were performed in 0.1 M perchloric acid ($HClO_4$) as supporting electrolyte, which was deoxygenated with argon gas one hour before use. This electrolyte solution does not hydrolyze the amide bonds of **1** adsorbed on gold. No hydrolysis products were observed in the STM images. All EC-STM imaging was performed at a work potential (V_W) of −100 mV *vs.* SCE electrode. At positive work potentials only a disordered phase was observed.

Tunnelling bias (V_t) and current (I_t) parameters were adjusted to achieve the highest possible resolution: V_t = −0.50 to −0.60 V, I_t = 1.0 nA for EC-STM experiments at the water/gold interface; V_t = −0.30 to −0.50 V, I_t = 0.60 nA for STM experiments at the 1-octanol/graphite interface.

STM images were analyzed using WSxM 4.0 (Nanotec Electronica S. L.) and SPIP 4.1 (Image Metrology) software.

Molecular modeling

Molecular modeling calculations were carried out using the compass force field, as implemented in Materials Studio, a product of Accelrys, San Diego, CA, USA. The energy minimizations were carried out in the gas phase with a dielectric constant of 1. All energy-terms were included with the exception of an explicit hydrogen-bonding term. For the non-bonding interactions a cut-off radius of 12.5 Å was used, with a spine width of 3 Å, and a buffer width of 1.0 Å. A graphite sheet, 20 × 30 atoms in size, with fixed Cartesian position for the carbon atoms was used as the substrate. All structures

were subjected to energy minimization using the Fletcher-Reeves algorithm, to a final gradient with maximum derivative of 0.001 kcal mol^{-1}. The folding ability was expressed by comparison of the total potential energy for the energy-minimized intramolecular H-bonded structure, with the optimized extended conformation without intramolecular hydrogen bond and with all CH_2–CH_2 bonds in *trans* configuration, and both conformations in close contact with the graphite substrate.

Acknowledgements

The authors thank the Federal Science policy through IUAP-V-03, the Institute for the promotion of innovation by Science and Technology in Flanders (IWT), and the Fund for Scientific Research-Flanders (FWO), as well as the Top Institute Material Science Center (MSC+) of the University of Groningen. A. S. K. thanks the Fund for Scientific Research-Flanders for financial support. We would like to thank Dr Peter Broekmann, Prof. Wandelt and their coworkers (University of Bonn) for their support and stimulating discussions.

References

1 M. O. Lorenzo, C. J. Baddeley, C. Muryn and R. Raval, *Nature*, 2000, **404**, 376.
2 (*a*) Y. Okawa and M. Aono, *Nature*, 2001, **409**, 683; (*b*) M. M. Akai-Kasaya, K. Shimizu, Y. Watanabe, A. Saito, M. Aono and Y. Kuwahara, *Phys. Rev. Lett.*, 2003, **91**, 255501; (*c*) A. Miura, S. De Feyter, M. M. S. Abdel-Mottaleb, A. Gesquière, P. C. M. Grim, G. Moessner, M. Sieffert, M. Klapper, K. Müllen and F. C. De Schryver, *Langmuir*, 2003, **19**, 6474; (*d*) S. Hoeppener, L. F. Chi and H. Fuchs, *Nano Lett.*, 2002, **2**, 459.
3 F. Jäckel, W. D. Watson, K. Müllen and J. P. Rabe, *Phys. Rev. Lett.*, 2004, **92**, 188303.
4 (*a*) J. Rabe and S. Buchholz, *Science*, 1991, **253**, 424; (*b*) D. M. Cyr, B. Venkataraman and G. W. Flynn, *Chem. Mater.*, 1996, **8**, 1600; (*c*) P. Samori, *J. Mater. Chem.*, 2004, **14**, 1353.
5 (*a*) T. A. Jung, R. R. Schlittler, J. K. Gimzewski, H. Tang and C. Joachim, *Science*, 1996, **271**, 181; (*b*) T. A. Jung, R. R. Schlittler and J. K. Gimzewski, *Nature*, 1997, **386**, 696; (*c*) H. B. Fang, L. C. Giancarlo and G. W. Flynn, *J. Phys. Chem. B*, 1999, **103**, 5712; (*d*) F. Tao, J. Goswami and S. Bernasek, *J. Phys. Chem. B*, 2006, **110**, 4199; (*e*) R. Azumi, E. Mena-Osteritz, R. Boese, J. Benet-Buchholz and P. Bauerle, *J. Mater. Chem.*, 2006, **16**, 728–735; (*f*) S. Weigelt, C. Busse, L. Petersen, E. Rauls, B. Hammer, K. V. Gothelf, F. Besenbacher and T. R. Linderoth, *Nat. Mater.*, 2006, **5**, 112; (*g*) A. Ziegler, W. Mamdouh, A. V. Heyen, M. Surin, H. Uji, M. M. S. Abdel-Mottaleb, F. C. De Schryver, S. De Feyter, R. Lazzaroni and S. Hoger, *Chem. Mater.*, 2005, **17**, 5670–5683; (*h*) B. A. Hermann, L. J. Scherer, C. E. Housecroft and E. C. Constable, *Adv. Funct. Mater.*, 2006, **16**, 221; (*i*) M. C. Lensen, S. J. T. van Dingenen, J. A. A. W. Elemans, H. P. Dijkstra, G. P. M. van Klink, G. van Koten, J. W. Gerritsen, S. Speller, R. J. M. Nolte and A. E. Rowan, *Chem. Commun.*, 2004, 762.
6 (*a*) D. J. Hill, M. J. Mio, R. B. Prince, T. S. Hughes and J. S. Moore, *Chem. Rev.*, 2001, **101**, 3893; (*b*) D. J. Hill and J. S. Moore, *Proc. Natl. Acad. Sci. U. S. A.*, 2002, **99**, 5053; (*c*) A. Khan, C. Kaiser and S. Hecht, *Angew. Chem., Int. Ed.*, 2006, **45**, 1878.
7 N. Schuurmans, H. Uji-i, W. Mamdouh, F. C. De Schryver, B. L. Feringa, J. vanEsch and S. De Feyter, *J. Am. Chem. Soc.*, 2004, **126**, 13884.
8 S. De Feyter and F. C. De Schryver, *J. Phys. Chem. B*, 2005, **109**, 4290.
9 (*a*) W. Mamdouh, H. Uji-i, J. Ladislaw, A. Dulcey, V. Percec, F. C. De Schryver and S. De Feyter, *J. Am. Chem. Soc.*, 2006, **128**, 317; (*b*) B. Venkataraman, J. J. Breen and G. W. Flynn, *J. Phys. Chem.*, 1995, **99**, 6608; (*c*) M. Lackinger, S. Griessl, W. M. Heckl, M. Hietschold and G. W. Flynn, *Langmuir*, 2005, **21**, 4984.
10 A. Gesquière, M. M. Abdel-Mottaleb, S. De Feyter, F. C. De Schryver, M. Sieffert, K. Müllen, A. Calderone, R. Lazzaroni and J.-L. Brédas, *Chem.–Eur. J.*, 2000, **6**, 3739.
11 (*a*) S. Yoshimoto, N. Higa and K. Itaya, *J. Am. Chem. Soc.*, 2004, **126**, 8540; (*b*) Z. Li, B. Han, L. J. Wan and T. Wandlowski, *Langmuir*, 2005, **21**, 6915; (*c*) C. Safarowsky, L. Merz, A. Rang, P. Broekmann, B. A. Hermann and C. A. Schalley, *Angew. Chem., Int. Ed.*, 2004, **43**, 1291; (*d*) T. Ye, Y. F. He and E. Borguet, *J. Phys. Chem. B*, 2006, **110**, 6141; (*e*) Q. H. Yuan and L. J. Wan, *Chem.–Eur. J.*, 2006, **12**, 2808.
12 K. Ienaga, K. Higashiura, Y. Toyomaki, H. Matsuura and H. Kimura, *Chem. Pharm. Bull.*, 1988, **36**, 70.
13 Moreover, most likely, the molecules are not folded with a side-on orientation. If side on, intermolecular hydrogen bonding will not be optimized. Furthermore, as the alkyl chains are not very transmissive for tunnelling electrons, having a double layer of alkyl chains could hamper high quality imaging of the adsorbed layer as the tip might interact with the 'upper alkyl chains' under the given experimental conditions.
14 J. Brinksma, B. L. Feringa, R. M. Kellogg, R. Vreeker and J. van Esch, *Langmuir*, 2000, **16**, 9249.
15 As the sample cell is not closed, the solvent evaporates too fast. Faradaic currents due to residual water mask the tunnelling current. Coating of the tip according to the procedure for EC-STM is also not ideal since ethanol might (partly) dissolve the coating.
16 S. Yoshimoto, R. Narita and K. Itaya, *Chem. Lett.*, 2002, 356.
17 As no clear images of the Au(111) lattice could be recorded, and therefore internal calibration is lacking, an accurate analysis of the parameters describing the molecular ordering is not provided.
18 M. Wilms, M. Kruft, G. Bermes and K. Wandelt, *Rev. Sci. Instrum.*, 1999, **70**, 3641.

